Received Date : 03-Dec-2015

Revised Date : 27-Apr-2016

Accepted Date : 04-May-2016

Article type : Original Article

Manuscript Category: Signaling & Cell biology (SCB)

Multiparameter analysis of naevi and primary melanomas identifies a subset of naevi with elevated markers of transformation

Carly Fox[1], Duncan Lambie[2], James S Wilmott[3], Alex Pinder[1], Sandra Pavey[1], Kim-Anh Lê Cao[1], Taner Akalin[4], Isil Kilinc Karaarslan[5], Fezal Ozdemir[5], Richard A Scolyer[3], Miko Yamada[6], H Peter Soyer[6], Helmut Schaider[6], Brian Gabrielli[1].

[1]The University of Queensland Diamantina Institute, Translational Research Institute, Brisbane, Australia. [2]IQ Pathology, Brisbane, Queensland, Australia. [3]Melanoma Institute Australia, Sydney, Australia. [4]Department of Pathology, Ege University, Bornova, 35100, Izmir, Turkey; [5]Department of Dermatology, Ege University, Bornova, 35100 Izmir, Turkey; [6]Dermatology Research Centre, The University of Queensland, School of Medicine, Translational Research Institute, Brisbane, Australia

Corresponding Author:

Professor Brian Gabrielli

The University of Queensland Diamantina Institute, Translational Research Institute, Brisbane, Australia 4102

Email: brianG@uq.edu.au

Running Title: Naevi with elevated risk

Summary

Here we have carried out a multiparameter analysis using a panel of 28 immunohistochemical markers to identify markers of transformation from benign and dysplastic naevus to primary melanoma in three separate cohorts totaling 279 lesions. We have identified a set of eight markers that distinguish naevi from melanoma. None of markers or parameters assessed differentiated benign from dysplastic naevi. Indeed, the naevi clustered tightly in terms of their immunostaining patterns whereas primary melanomas showed more diverse staining patterns. A small subset of histopathologically benign lesions had elevated levels of multiple markers associated with melanoma, suggesting that these represent naevi with an increased potential for transformation to melanoma.

Significance

Up to 50% of melanomas are derived from naevi, although the potential for an individual naevus to transform to melanoma is exceedingly low. The question of which naevi have the potential to transform to melanoma is currently based on clinical guidelines and the experience of the clinician. There is currently no evidence for the existence of naevi that have

accumulated molecular alterations normally associated melanoma, and thus represent a potential reservoir of high risk pre-cancers. Here we have investigated known markers associated melanoma formation and identified a subset of naevi that appear to have elevated transformation potential.

Introduction

Despite the recent advances in treatment, 5 year survival in late stage melanoma remains very low, but if it is detected early, melanoma is curable. Current clinical practice relies on the detection of early melanoma and changing naevi – a clue that malignant transformation of melanocytes to melanoma is underway. Whilst the phenotypic features of this transformation are well recognized, the molecular mechanisms underlying these changes remain elusive.

There are divergent pathways for the development of melanoma, those that develop on chronically sun exposed sites, and those on sites of intermittent exposure (Whiteman et al., 2003). The latter are associated with BRAF, and to a slightly lesser extent NRAS mutations, and increased nevus counts (Walker, 2008), with high numbers of naevi (>60) being one of the strongest risk factors for the development of melanoma. While 20-50% of melanomas develop from naevi, few become melanoma and clinically it is difficult to predict which naevus is likely to undergo neoplastic change. This is particularly important for high-risk dysplastic naevus syndrome (DNS) patients where excision of all naevi is not feasible. The ability to identify and treat naevi which were likely to become melanoma could significantly reduce melanoma rates in the general population, particularly the high risk DNS population. The clinical problem is to identify the naevi with high transformation potential for treatment. The existence of a population of "partially transformed" naevi has not been demonstrated as

these lesions will have a similar appearance on normal histopathological assessment as benign lesions. However, at the molecular level they are likely to have altered pathways that could contribute to neoplastic transformation, but dysregulation of other pathways to drive transformation. Multiple molecular pathways have been implicated in the pathogenesis of melanoma, but the temporal and spatial sequence of events is not well established. Like many cancers, melanoma is thought to result from the accumulation of genetic alterations within a single cell, until it attains malignant potential. Alterations in the p16/CDK4/RB (Castellano et al., 1997) and MAP kinase pathways (de Snoo and Hayward, 2005; Hodis et al., 2012), PI3K, p53 (Avery-Kiejda et al., 2011), and β-Catenin/Notch (Bachmann et al., 2005) pathways have been described. Many of these altered pathways have also been report in naevi. For example, either oncogenic *NRAS* or *BRAF* mutations are present in the majority of naevi, although a significant proportion of melanomas are wild type for both these genes (Hodis et al., 2012; Pollock et al., 2003). Thus, individually altered pathways associated with melanoma can be insufficient to indicate the transformation potential of an individual naevus.

Many previous studies have identified single markers that are implicated in the progression to melanoma. However, very few studies have used large-scale tissue microarray analysis to determine the role of a panel of markers in malignant transformation. Here we have examined differential expression of 28 molecular markers from pathways previously implicated in melanoma development, to investigate whether there is a subset of histologically benign naevi that expressed markers associated with transformation to melanoma. Using our observations from the staining patterns of these molecular markers, we have defined a set of markers that differentiate between naevi and melanomas, and identified a small proportion of naevi with alterations of a subset of markers that are normally strongly associated with transformation.

Results

Markers of Transformation

To identify markers that discriminate between pre-malignant naevus and the transformed state of primary melanoma, we assessed a total of 28 molecular markers using tissue microarrays to refine a large set of tumour intrinsic markers. The useful markers from this screen were validated on a set of full width lesions, with an additional set of microenvironment localised markers identified from the literature with potential to discriminate between naevus and melanoma. The most discriminatory set of markers from this analysis where then further validated in an independent set of full width lesions (Supplementary Figure S1). A total of 21 markers identified in the literature as being altered during progression to melanoma were initially assessed for their ability to discriminate between naevus and melanoma using tissue microarrays representing the spectrum from benign naevus to metastatic melanoma (Supplementary Table S1). A number of these markers (FAPB-7, γ-H2Ax, APE1, p53, Cyclin D1, COX2, phospho-STAT3, Survivin and MITF) failed to discriminate between naevus and primary melanoma, and were thus excluded from further analysis. The remaining 12 markers were assessed semi-quantitatively using a larger TMA with 100 lesions represented in three cores each lesion. The number of samples and their diagnosis is shown in Supplementary Table S2 and S3.

Initial inspection revealed that for the majority of markers, there was little difference in the staining of benign and dysplastic naevus. This was clearly demonstrated by a comparison of H Scores for these markers (Supplementary Figure S2A, B). The univariate analysis identified nine markers significantly different between the combined naevus (benign, dysplastic) and primary melanoma (thin, thick; Supplementary Table S4; false discovery rate (FDR) ≤ 0.05). To complement this analysis, the multivariate statistical method random

Forest identified these same parameters as the strongest discriminators, although in a slightly different order (Supplementary Figure S3). However, when the H Scores for each marker were assessed for each diagnosis category, the majority of these revealed that they most changed between thin and thick primary melanomas (Supplementary Figure S2A, B). Five of these markers were strongly associated with thick melanomas, lymph node and distant metastasis, including β-Catenin, E-Cadherin and c-KIT which decreased in total intensity, and Nestin and MCAM which increased in intensity from thin to thick melanoma. BRN2 and CDK6 were more weakly associated with this latter trend. This pattern of expression suggested that these are likely to represent markers of increased tumor growth and/or metastasis. The markers with the strongest correlation with the transformation from dysplastic nevus to thin primary melanoma were p16 and HMGB2, both of which had reduced staining associated with transformation. Typical staining patterns p16 and HMGB2 in naevus and thin melanomas are shown in Figure 1, and typical staining for a selection of other markers in the TMAs is shown in Supplementary Figure S4.

The eight most informative markers from the TMA analysis, including c-KIT, β-Catenin, and BRN2, were taken forward to further analysis in a separate panel of 95 full-width lesion representing the spectrum from benign naevus to thick melanoma. An additional seven markers identified from the literature including stromal markers such as D240/podoplanin as a marker of lymph angiogenesis, and CD31 for angiogenesis, were also assessed. The markers assessed, numbers and diagnosis of lesions in this set is reported in Supplementary Table S5 and S6. Examples of the typical staining pattern for each marker in naevus and melanoma are shown in Supplementary Figure S5.

Preliminary analysis of the additional markers showed N-Cadherin, PTEN, Ki67 and D240 strongly discriminated between naevus and melanoma with p values < 0.0001 (Mann Whitney test). BRaf V600E staining revealed the expected frequency in each diagnosis, with 62% of nevus (35/57) and 38% melanomas (15/39) staining positive. Univariate statistical analysis of all the naevi versus all melanomas combined provided very similar results to analysis of dysplastic naevi versus thin melanomas only, thus only the latter analysis is shown (Table 1). This revealed the number of D240 lymphatic vessels was one of the strongest indicators of transformation along with gain of nuclear N-Cadherin and loss of PTEN staining, absence of nuclear β-Catenin and p16 staining, increased CD68 macrophages and loss of HMGB2 staining. The gain or loss of nuclear N-Cadherin, p16 and β-Catenin were independent of the staining intensity of these markers.

Unsupervised multivariate analysis with multiple Correspondence Analysis (MCA) based on all significant staining parameters identified previously showed that naevi were clustered away from the thin and thick primary melanomas, with the in situ melanomas clustering across these two groups (Figure 2). Along the first MCA component, the majority of naevi, benign and dysplastic, clustered tightly whereas the melanomas although clearly separated from naevi, were more dispersed, indicating a significant degree of divergence in their staining patterns. The second MCA component highlighted a subset of naevi that did well separate from the majority of naevi, indicating significant divergence from the normal staining of naevi, and have acquired some of the changes associated with melanomas.

Prior to Random Forest statistical analysis, the continuous variable Ki67 and D240 were converted to categorical variables to enable this analysis (Supplementary Figure S6). While this cut off provided a clear distinction between naevus and melanoma with Ki67

staining, it was more ambiguous for D240. Random Forest analysis identified the same set of strongly discriminatory markers in separate analysis of the combined naevi versus combined melanomas, and dysplastic naevi versus thin primary melanomas, although in a slightly different order. Stability analysis likewise demonstrated that Ki67, gain of N-Cadherin nuclear staining, PTEN % cells and score, loss of β-Catenin and p16 nuclear staining were the strongest discriminators of transformation to melanoma from dysplastic naevus. Combined, these parameters had a sensitivity of 93% and specificity of 79%, with an error rate of 13% (Supplementary Table S7).

Another feature of the skin sections that was readily discerned was the degree of elastosis. Scoring the lesions for elastosis revealed a significant degree of difference between the naevus and melanoma groups, with the majority of naevi showing Elastosis scores 1-2 while the primary melanomas had a greater range but overall a higher Elastosis score (Supplementary Figure S7A). A high proportion of the higher Elastosis scores were associated with lesions from areas of chronic sun damage, but this was not exclusively the case. There were differences in average ages of the naevus and melanoma patients as expected, with the naevus average of 43.5 ±18 y, and melanoma 63.8 ± 17 y. This corresponded to the difference in solar elastosis score of naevus 1.4 ±0.7 and melanoma 2.6 ±1.1 ($p < 0.0001$). There were no differences based on sex, and the differences in immunostaining and solar elastosis were independent of age of the subject.

These top eight discriminating parameters, plus the Elastosis score were assessed to determine the minimal number of parameters required to predict transformation. The PTEN % cells, score and nuclear localization were combined as the H score to reduce this to seven parameters (Table 2; Figure 3). The Elastosis score was a significant discriminator between

naevus and melanoma (Supplementary Figure S7B). We established a Transformation score to each lesion, where a score of 1 was assigned in the following cases: 3 or more D240 vessels, score of 2 or more Ki67, PTEN H score ≤ 4, the presence of nuclear N-Cadherin staining, absence of nuclear p16, absence of nuclear β-Catenin staining, and elastosis score greater than 1 to give a maximum score of seven (Table 2). It was found that 32/36 (89%) of melanomas had a score of four or more, whereas only 4/57 (7%) of naevus had a Transformation score of 4 or more (Figure 4A). The four melanomas with a score less than four all had ≤ 2% Ki67 positive cells, nuclear β-Catenin, no nuclear N-Cadherin and elevated PTEN levels, indicating weakly proliferating/indolent melanomas. The highest scoring naevi had lost nuclear β-Catenin, gained nuclear N-Cadherin, but retained nuclear p16. These may represent naevi with a strong potential for transformation. Addition of the BRAF mutation status did not increase the power of these features to discriminate between nevus and melanoma.

This seven marker set was analysed in a separate validation set of 62 full width lesions representing naevus and primary melanoma (Supplementary Table S8 and S9). These were stained with the six markers identified above and for elastosis, scored, and the Transformation score calculated based on the same parameters as in Table 2. Again there was a significant difference between naevi and melanomas (Figure 4B). The higher scoring naevi (3-5) had high elastosis scores and ≤ 2% Ki67 positive cells suggesting higher levels of sun exposure and a more highly proliferative state (Figure 4B), whereas the lower scoring melanomas (3) often had low elastosis scores and no nuclear N-Cadherin. Random forest analysis was performed on the pooled naevi (benign and dysplastic) and melanomas (in situ and primary) for identifying naevus and melanoma. This produced a 16% classification error rate, all the misclassified lesions were naevi, classified as melanoma (Table 3). The

significance of the difference in Transformation scores for the pooled naevi and pool melanomas for both data sets was $p < 0.0001$ (Mann Whitney U test).

Discussion

Here we have assessed a large panel of previously identified markers of transformation to melanoma to determine whether multiparameter analysis of melanocytic lesions could better identify naevi that displayed markers normally associated with the transformation to melanoma. We have shown using seven markers, including the level of solar elastosis as a surrogate marker of UV exposure, that when combined they discriminated between naevi and thin primary melanomas. This set of markers was demonstrated to have discrimination in an independent validation set of melanocytic lesions. Although these markers may be useful in providing a molecular signature of melanoma, it was clear that they did not perform significantly better than conventional histopathologic diagnosis. However, the study did provide useful insights into the different classifications currently used for these melanocytic lesions, and more importantly identified a subset of histopathologically benign naevi that had accumulated markers strongly associated with the transformed phenotype.

A number of features stood out from this study. The first was that with the large panel of markers used in this study it was not possible to discriminate between benign and dysplastic naevi. The classification of dysplastic naevus is controversial, and recently the justification for such a classification has been questioned (Hurwitz and Tavel, 2015; Rosendahl et al., 2015). Currently, dysplastic naevi are defined clinically as well as histopathologically based on the original work of Elder in 1980 (Elder et al., 1980). However, the majority of epidemiological studies do not discriminate between benign and

dysplastic naevi, and these studies provide evidence for an increased number of naevi associate with increased melanoma risk (Olsen et al., 2010; Usher-Smith et al., 2014). The number, morphology and type of naevi is a strong indicator of melanoma risk, with 42% of people with high mole counts (>60) developing melanoma (Olsen et al., 2010), and 20-50% melanomas arise from pre-existing naevi (Goldstein and Tucker, 2013). There are likely to be differences in gene expression associated with dysplastic features, although whether this remains a useful diagnosis in terms of melanoma risk is less certain. The set of most discriminatory markers represent genes with known contribution to melanoma transformation. $BRAF^{V600E}$ expression in melanocytes induces p16 expression, a major factor in the senescence phenotype and proliferative arrest (Gray-Schopfer et al., 2006; Michaloglou et al., 2005). Activation of PI3K-ATK pathway, commonly through mutation/down-regulated expression of PTEN (Dankort et al., 2009; Vredeveld et al., 2012) or increased AKT3 (Cheung et al., 2008) bypasses OIS and promotes tumorigenesis. Thus loss of PTEN and nuclear p16 are expected contributors to transformation. Increased N-Cadherin has been associated with loss of PTEN signalling (Lade-Keller et al., 2013), and the loss of nuclear β-Catenin may be related to gain of nuclear N-Cadherin (Grossmann et al., 2013). Although the accumulation of nuclear β-Catenin is commonly associated with transformation in many cancer types, its role in melanoma is less clear (Webster and Weeraratna, 2013). Loss of nuclear β-Catenin has been observed previously in melanomas (Bachmann et al., 2005). The reciprocal nature of nuclear β-Catenin and N-Cadherin was a common, but not a invariable, feature in the lesions examined in the current study. The association of transformation with increase lymphangiogenesis (D240 vessels) is unclear. The Ki67 staining was also of interest particularly in the naevi. It appeared that the higher the number of more transformation markers accumulated by a naevus, the higher the chance of

there being evidence of proliferation. Unsurprisingly, all of the melanomas with very few exceptions were highly proliferative.

This data indicates that although naevus transformation to melanoma is an uncommon event (the overall risk of any individual naevus developing into a melanoma ~1/30,000 (Tsao et al., 2003)), naevi represent a reservoir of premalignant cells. The immunostaining also showed that in the majority of cases, the changes in marker staining were relatively uniform across the naevi, only in few cases was staining found to be localised to parts of a naevus. Thus the naevus represents a large reservoir of premalignant cells that require few further changes/mutations to acquire a fully transformed phenotype. This is likely to be a multistep process rather than any single event being responsible for transformation. There are also likely to be multiple pathways that can lead from naevus to melanoma. This is apparent from the spread of melanoma staining patterns shown in the MCA analysis compared with the much tighter clustering of the naevus staining patterns. For example, multiple pathways have been identified that can bypass BRAF/NRAS induced senescence, a major obstacle to transformation. These including metabolic rewiring through pyruvate dehydrogenase (PDH) (Kaplon et al., 2013), up-regulation of ribonucleotide reductase subunit M2 (RRM2) which is rate limiting for dNTP synthesis (Aird et al., 2013), increased mTOR signalling (Damsky et al., 2015), and activation of the PI3K-ATK pathway (Cheung et al., 2008; Dankort et al., 2009; Vredeveld et al., 2012). Dysregulation of any of these pathways could drive past the senescence arrest to promote transformation to melanoma, although it is likely that multiple pathways are involved.

The existence of a subset of histologically benign naevi with elevated markers of transformation suggests that if a non-invasive means of identifying these can be developed, it may be present clinicians with an opportunity to focus their treatment decisions on these higher risk lesions. This should translate into improved outcomes and less unnecessary excisions, particularly in high risk DNS population.

Materials and Methods

Selection of immunohistochemical markers

A candidate gene approach based on extensive literature review was used to select a panel of 20 potential molecular markers of transformation. Markers required a commercially available antibody for detection in formalin-fixed, paraffin embedded tissue. Selected markers had been previously implicated in the transformation to melanoma and covered a spectrum of roles in melanoma pathogenesis including markers of proliferation, cell differentiation, and structural proteins. The markers selected and antibodies used are reported in Supplementary Table S10.

Immunohistochemistry

Slides were deparaffinized and rehydrated through xylene to water. Antigen retrieval was performed with a five minute boiling cycle in 0.01M citrate buffer in a commercial decloaker. Peroxidase block was performed with 3% hydrogen peroxide for 15 minutes. Non-specific binding was blocked with donkey serum/bovine serum albumin in TBS for 30 minutes prior to overnight incubation with the primary antibody. The immunohistochemistry procedure was performed using an IMPRESS universal kit (Vector) according to the manufacturer's guidelines. Vector ImmPACT NovaRED peroxidase substrate was applied as a chromogen

for visualization of the immunoreaction. Haematoxylin was used for counterstain. Negative controls were obtained by omitting the primary antibody. Positive controls were obtained using tissue sections known to be positive for the antibody in use. Specific staining by each of the antibodies assessed here was initially validated with the positive control tissue arrays, and positive controls were included for each antibody in conjunction with the TMA staining. Additionally, normal human skin (neonatal foreskin) was used a further control for normal skin staining of melanocytes and provide an indication of intensity of staining. Slides were mounted using ClearMount mounting solution (Invitrogen) and coverslipped with Xylene and Entellan (Merck Millipore) mounting media. They were then scanned using an Aperio slide scanner at 20x magnification.

Immunohistochemistry Scoring

Two experienced dermatopathologist (HPS and DL) independently reviewed biopsies in the initial set of 95 full width lesions. In the few cases where there was disagreement in the diagnosis, they consulted to come to a consensus. DL also independently reviewed the diagnosis of the TMA samples. Two independent observers (BG, DL) performed a blinded evaluation of the immunohistochemically stained slides. Each antibody was scored according to a defined set of parameters specific to that marker. Overall intensity of immunoreactivity was evaluated using a stepwise scoring system (0 to 3+): 0 (negative): no staining; 1+/-: very weak staining; 2+ weak staining; 3+ moderate staining; or 4+ strong staining. Percentage of immunoreactive cells was evaluated using a stepwise scoring system (0-100%); 0: no cells stained; 1: 1-33% of cells stained; 2: 33-66% of cells stained; 3: >66% of cells stained. Nuclear, cytoplasmic and membranous staining were allocated a score of 0 or 1 indicating staining to be present or absent. TMA spots with a lack of tumor tissue or presence of necrosis or crush artifact were excluded from the analysis. In case of discordant scoring

results a consensus score was assigned. Features scored with each of the markers used is presented in Supplementary Table S11. H scores were calculated as the product of the categorised intensity and categorised percentage cells stained.

Tissue Microarray Analysis

The TMA utilized in our study comprised 100 lesions, ranging from compound naevus to distant melanoma metastases The TMA consisted of triple-punch samples from formalin-fixed, paraffin-embedded lesions through Melanoma Institute Australia (MIA; Supplementary Table S3). Lesions were categorized for analysis into six ordered classes; benign naevus, dysplastic naevus, thin melanoma (<1mm), thick melanoma (>1mm), lymph node metastasis and distant metastasis, based on histologic examination of the full width lesions undertaken at Melanoma Institute Australia. Markers that were qualitatively informative from the initial TMA analyses were tested across this TMA, as well as a selection of additional markers identified in our literature search. Marker assessments using the TMAs are reported in Supplementary Table S11.

Full width section analysis

A series of 35 lesions was obtained from TA, MT, IKK, FO in Turkey. This set comprised 35 naevi on a spectrum of severely dysplastic to melanoma in situ and thin invasive melanoma. A series of 65 lesions was obtained from the Princess Alexandra Pathology Archives and 17 lesions were obtained from MyLab Pathology (DL), and a separate validation cohort 62 lesions were obtained from IQ Pathology (DL). Any melanocytic lesion excised in the past two years was considered for inclusion and lesions diagnosed as benign naevus, dysplastic naevus, thin or thick melanoma based on the reporting pathologist's diagnostic report were selected randomly. Lesions were included if there was sufficient tissue to permit sectioning

and immunohistochemical analysis. Histopathologic diagnosis was obtained by two authors' (HPS, DL) review of the original H&E-stained sections in conjunction with pertinent demographic and clinical information ascertained from the available surgical pathology report. Lesions were diagnosed as benign naevi, dysplastic naevi, melanoma in situ, thin melanoma (<1mm) or thick melanoma (>1mm), or other. All tissue samples were acquired following ethics approval from the University of Queensland (ref: 2011001201). Specimen details are included in Supplementary Table S12. Only informative immunohistochemical markers in the tissue microarray study were examined. Several new markers were included. CD31 and D240 were not tested on the TMA as these are extratumoral markers and their expression is seen in the stroma surrounding the lesion – tissue that is not included in a microarray sample. In addition, Osteopontin (OPN), Ki67, N-Cadherin, BRAF V600E and PTEN were not tested on the TMA due to limited availability of TMA material. Markers tested across the full-width specimen set are shown in Supplementary Table S5.

Data preprocessing

A common problem in large-scale immunohistochemical studies is missing values in the data matrix due to missing or damaged tissue specimens. In this study, 9.3% of values were missing. Patient data with missing data points was excluded from the analysis. Prior to analysis, p16 score and p16 % cells were converted to a binary scale (0,1) such that whenever values are ≥1 they were changed to a value of 1. These changes were made to better reflect the biology of p16 in that it is either present or absent in melanocytic lesions.

Statistical Analysis

Statistical analyses were conducted using the R statistical software version 2.11 using both univariate and multivariate statistical methods. For each categorical variable Fisher's exact univariate tests were performed to test the association between the counts observed in each category of the variable of interest, and the outcome (lesion diagnoses). For continuous variables (e.g. D240 vessels, Ki67), a non parametric Mann-Whitney test was performed to test the difference in medians between the different lesion diagnoses. P-values from those univariate tests were corrected using the Benjamini and Hochberg (Benjamini and Hochberg, 1995) approach to control the false discovery rate (FDR).

Multivariate analyses were performed on all categorical variables only. For those analyses, the variable Ki67 and D240 were converted to categorical variables by selecting obvious cutoff points in plots of data distribution blinded for lesion diagnosis. Cut offs of three D240 vessels per 10X high powered field, and 2% Ki67 positive nuclei were chosen (Supplementary Figure S5). Supervised multivariate analyses were performed using the Machine Learning approach Random Forest (RandomForest R package) (Breiman, 2001; Liaw, 2002) in order to identify biomarkers discriminating the different lesions, or assess the discriminative ability of the Transformation score. The top discriminate biomarkers were ranked according to a predictive accuracy measure as a direct output from the random forest analysis. A stability analysis was then performed using 10-fold cross-validation repeated 100 times to assess whether those top biomarkers were repeatedly selected across those runs. Unsupervised multivariate analysis was performed using Multiple Correspondence Analysis (MCA) (Greenacre, 2007), the counterpart of Principal Component Analysis for categorical variables, as a mean to cluster the lesions with no a priori on their diagnosis. MCA was based

on significant staining parameters previously identified in the univariate and Random Forest analyses.

Disclosure/Conflict of Interest

The authors have no disclosures or conflict of interest to declare.

Acknowledgements

The authors acknowledge the assistance of Xin-Yi Chua from QFAB for her assistance with the biostatistics. CF was supported by an Australia Postgraduate Award. BG is an NHMRC Senior Research Fellow. This work was supported by funding from the National Health and Medical Research Council of Australia and the Cancer Council Queensland.

References

Aird, K. M., Zhang, G., Li, H., Tu, Z., Bitler, B. G., Garipov, A., Wu, H., Wei, Z., Wagner, S. N., Herlyn, M., et al. (2013). Suppression of nucleotide metabolism underlies the establishment and maintenance of oncogene-induced senescence. Cell Rep. *3***,** 1252-65.

Avery-Kiejda, K. A., Bowden, N. A., Croft, A. J., Scurr, L. L., Kairupan, C. F., Ashton, K. A., Talseth-Palmer, B. A., Rizos, H., Zhang, X. D., Scott, R. J., et al. (2011). P53 in human melanoma fails to regulate target genes associated with apoptosis and the cell cycle and may contribute to proliferation. BMC Cancer. *11:203.***,** 10.1186/1471-2407-11-203.

Bachmann, I. M., Straume, O., Puntervoll, H. E., Kalvenes, M. B., and Akslen, L. A. (2005). Importance of P-cadherin, beta-catenin, and Wnt5a/frizzled for progression of melanocytic tumors and prognosis in cutaneous melanoma. Clin Cancer Res. *11***,** 8606-14.

Benjamini, Y., and Hochberg, Y. (1995). Controlling the False Discovery Rate: A Practical and Powerful Approach to Multiple Testing. Journal of the Royal Statistical Society. Series B (Methodological) *57***,** 289-300.

Breiman, L. (2001). Random Forests. . Machine Learning *45***,** 5-32.

Castellano, M., Pollock, P. M., Walters, M. K., Sparrow, L. E., Down, L. M., Gabrielli, B. G., Parsons, P. G., and Hayward, N. K. (1997). CDKN2A/p16 is inactivated in most melanoma cell lines. Cancer Res *57***,** 4868-75.

Cheung, M., Sharma, A., Madhunapantula, S. V., and Robertson, G. P. (2008). Akt3 and mutant V600E B-Raf cooperate to promote early melanoma development. Cancer Res. *68***,** 3429-39.

Damsky, W., Micevic, G., Meeth, K., Muthusamy, V., Curley, D. P., Santhanakrishnan, M., Erdelyi, I., Platt, J. T., Huang, L., Theodosakis, N., et al. (2015). mTORC1 Activation Blocks Braf(V600E)-Induced Growth Arrest but Is Insufficient for Melanoma Formation. Cancer Cell. *27***,** 41-56.

Dankort, D., Curley, D. P., Cartlidge, R. A., Nelson, B., Karnezis, A. N., Damsky, W. E., Jr., You, M. J., Depinho, R. A., Mcmahon, M., and Bosenberg, M. (2009). Braf(V600E) cooperates with Pten loss to induce metastatic melanoma. Nat Genet. *41***,** 544-52.

De Snoo, F. A., and Hayward, N. K. (2005). Cutaneous melanoma susceptibility and progression genes. Cancer Lett *230***,** 153-86.

Elder, D. E., Goldman, L. I., Goldman, S. C., Greene, M. H., and Clark, W. H., Jr. (1980). Dysplastic nevus syndrome: a phenotypic association of sporadic cutaneous melanoma. Cancer. *46***,** 1787-94.

Goldstein, A. M., and Tucker, M. A. (2013). Dysplastic nevi and melanoma. Cancer Epidemiol Biomarkers Prev. *22***,** 528-32.

Gray-Schopfer, V. C., Cheong, S. C., Chong, H., Chow, J., Moss, T., Abdel-Malek, Z. A., Marais, R., Wynford-Thomas, D., and Bennett, D. C. (2006). Cellular senescence in naevi and immortalisation in melanoma: a role for p16? Br J Cancer *95***,** 496-505.

Greenacre, M. (2007). Correspondence Analysis in Practice, Chapman & Hall/CRC).

Grossmann, A. H., Yoo, J. H., Clancy, J., Sorensen, L. K., Sedgwick, A., Tong, Z., Ostanin, K., Rogers, A., Grossmann, K. F., Tripp, S. R., et al. (2013). The small GTPase ARF6 stimulates beta-catenin transcriptional activity during WNT5A-mediated melanoma invasion and metastasis. Sci Signal. *6***,** ra14.

Hodis, E., Watson, I. R., Kryukov, G. V., Arold, S. T., Imielinski, M., Theurillat, J. P., Nickerson, E., Auclair, D., Li, L., Place, C., et al. (2012). A landscape of driver mutations in melanoma. Cell. *150***,** 251-63.

Hurwitz, R. M., and Tavel, M. E. (2015). The mythical concept and untoward consequences of a diagnosis of dysplastic nevus: an overdue tribute to A. Bernard Ackerman, MD. Dermatology Practical & Conceptual *5***,** 31-34.

Kaplon, J., Zheng, L., Meissl, K., Chaneton, B., Selivanov, V. A., Mackay, G., Van Der Burg, S. H., Verdegaal, E. M., Cascante, M., Shlomi, T., et al. (2013). A key role for mitochondrial gatekeeper pyruvate dehydrogenase in oncogene-induced senescence. Nature. *498***,** 109-12.

Lade-Keller, J., Riber-Hansen, R., Guldberg, P., Schmidt, H., Hamilton-Dutoit, S. J., and Steiniche, T. (2013). E- to N-cadherin switch in melanoma is associated with

decreased expression of phosphatase and tensin homolog and cancer progression. Br J Dermatol. *169*, 618-28.

Liaw, A., Wiener, M. (2002). Classification and Regression by random Forest. R News *2*, 18-22.

Michaloglou, C., Vredeveld, L. C., Soengas, M. S., Denoyelle, C., Kuilman, T., Van Der Horst, C. M., Majoor, D. M., Shay, J. W., Mooi, W. J., and Peeper, D. S. (2005). BRAFE600-associated senescence-like cell cycle arrest of human naevi. Nature *436*, 720-4.

Olsen, C. M., Carroll, H. J., and Whiteman, D. C. (2010). Estimating the attributable fraction for cancer: A meta-analysis of nevi and melanoma. Cancer Prev Res (Phila) *3*, 233-45.

Pollock, P. M., Harper, U. L., Hansen, K. S., Yudt, L. M., Stark, M., Robbins, C. M., Moses, T. Y., Hostetter, G., Wagner, U., Kakareka, J., et al. (2003). High frequency of BRAF mutations in nevi. Nat Genet. *33*, 19-20.

Rosendahl, C. O., Grant-Kels, J. M., and Que, S. K. T. (2015). Dysplastic nevus: Fact and fiction. Journal of the American Academy of Dermatology *73*, 507-512.

Tsao, H., Bevona, C., Goggins, W., and Quinn, T. (2003). The transformation rate of moles (melanocytic nevi) into cutaneous melanoma: a population-based estimate. Arch Dermatol. *139*, 282-8.

Usher-Smith, J. A., Emery, J., Kassianos, A. P., and Walter, F. M. (2014). Risk prediction models for melanoma: a systematic review. Cancer Epidemiol Biomarkers Prev. *23*, 1450-63.

Vredeveld, L. C., Possik, P. A., Smit, M. A., Meissl, K., Michaloglou, C., Horlings, H. M., Ajouaou, A., Kortman, P. C., Dankort, D., Mcmahon, M., et al. (2012). Abrogation of

BRAFV600E-induced senescence by PI3K pathway activation contributes to melanomagenesis. Genes Dev. *26***,** 1055-69.

Walker, G. (2008). Cutaneous melanoma: how does ultraviolet light contribute to melanocyte transformation? Future Oncol. *4***,** 841-56.

Webster, M. R., and Weeraratna, A. T. (2013). A Wnt-er migration: the confusing role of beta-catenin in melanoma metastasis. Sci Signal. *6***,** pe11.

Whiteman, D. C., Watt, P., Purdie, D. M., Hughes, M. C., Hayward, N. K., and Green, A. C. (2003). Melanocytic nevi, solar keratoses, and divergent pathways to cutaneous melanoma. J Natl Cancer Inst. *95***,** 806-12.

Tables:

Table 1: Univariate analysis of marker of naevus transformation to thin primary melanoma

	Variable	**Test**	**p-value**	**Association with malignant phenotype**
1	D240 vessels	Mann-Whitney	1.87E-23	Increase number of vessels per 10X hpf
2	PTEN % cells	Fisher's exact	1.09E-08	Loss of % cells stained
3	N-Cadherin nuclear	Fisher's	2.20E-08	Increase in nuclear staining
4	PTEN score	Fisher's	4.09E-07	Loss of intensity of staining
5	Ki67	Mann-Whitney	5.27E-07	Increased % cells stained
6	β-Catenin nuclear	Fisher's	1.42E-05	Loss of nuclear staining
7	p16 nuclear	Fisher's	1.75E-04	Loss of nuclear staining
8	N-Cadherin % cells	Fisher's	9.47E-03	Increase in % cells stained
9	N-Cadherin score	Fisher's	1.17E-02	Increase in intensity of staining
10	HMGB2 score	Fisher's	4.17E-02	Loss of intensity of staining
11	CD68 number of cells	Fisher's	4.21E-02	Increase in number of cells per10X hpf

Table 2: Transformation score. Parameters used to identify transformed melanoma. The Transformation score is the sum of the seven individual scores, where a score of 1 was assigned in the following cases: 3 or more D240 vessels, score of 2 or more Ki67, PTEN H score ≤ 4, the presence of nuclear N-Cadherin staining, absence of nuclear p16, absence nuclear β-Catenin staining, and elastosis score greater than 1 to give a maximum score of seven.

	Variable	**Score = 1 if**
1	D240 vessels	≥ 3
2	Ki67	≥ 2
3	PTEN H score	< 4
4	N-Cadherin nuclear	yes
5	β-Catenin nuclear	no
6	p16 nuclear	no
7	Elastosis score	>1

Table 3: Random Forest analysis to assess the combined seven marker Transformation score ability to discriminate and predict naevus and melanoma. Analysis was performed on the pooled naevi and pooled melanomas. Classification error rate was 16% as detailed in the contingency matrix (real classes indicated in rows, and random forest predictions based on 500 bootstrap trees indicated in columns).

	Naevus	**Melanoma**
Naevi	22	10
Melanomas	0	30

Titles and legends to figures

Figure 1:

Typical staining patterns for p16 and HMGB2 in naevus and thin primary melanomas. In both cases, there is a reduction in the strong nuclear staining in the melanomas.

Figure 2:

MCA sample plot showing only the samples coloured according to diagnosis type (1, benign naevus; 2, dysplastic naevus; 3 melanoma in situ; 4, thin primary melanoma; 5, thick primary melanoma). Types 1-2 can be well separated from Types 4-5 using the first component (x-axis), while Type 3 samples are spread across the two clusters.

Figure 3:

Typical staining pattern for the indicated markers in naevi and thin primary melanomas.

Figure 4:

Transformation score calculated for each lesion in the learning (A) and validation sets (B) using the criteria in Table 2. The colored marks indicated the percentage of Ki67 positive cells in each lesion. * $p<0.05$, ** $p<0.005$, *** $p<0.001$.

Figure 1

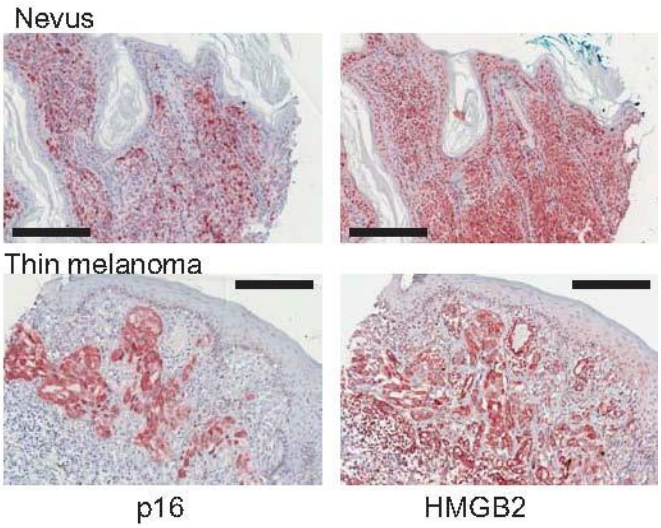

Figure 2

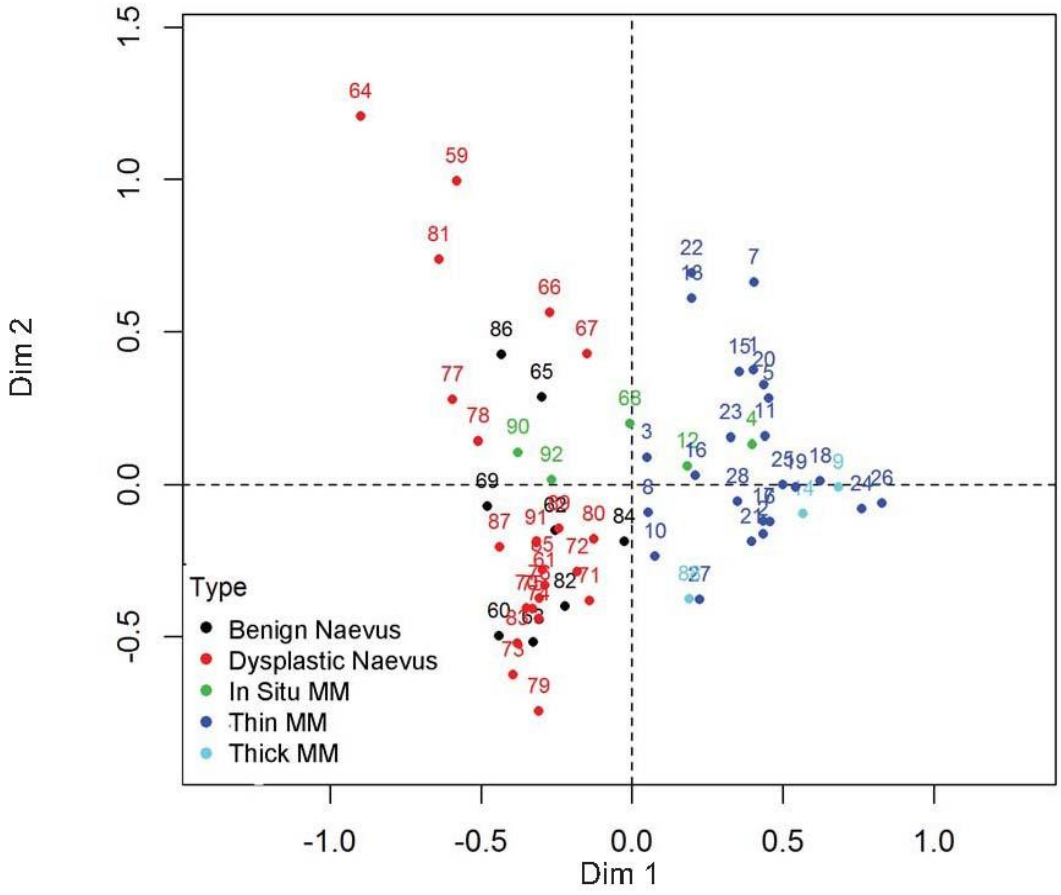

Figure 3

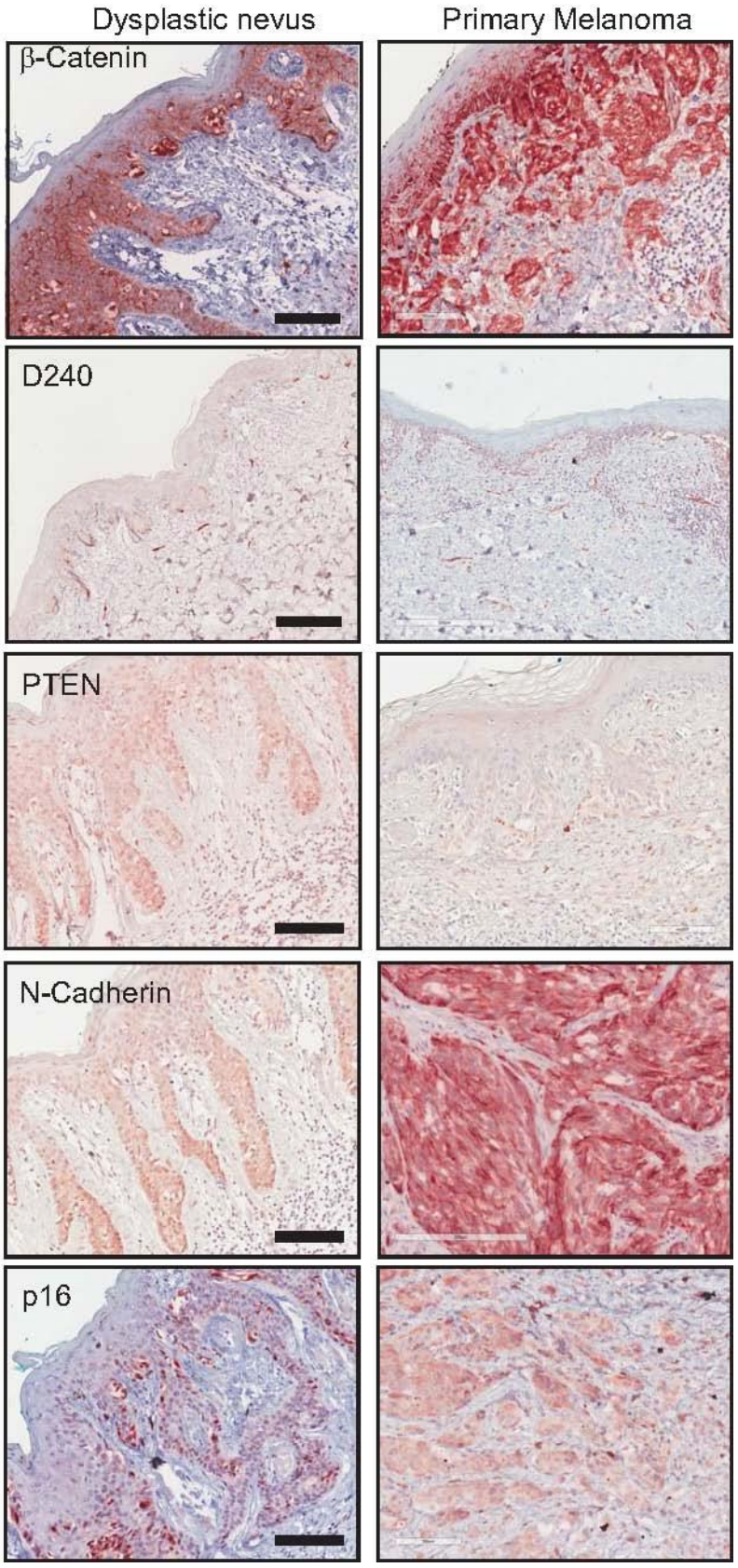

Figure 4